



1 **Divergent responses of evergreen needle-leaf forests in Europe to the 2020 warm winter**

2

3 Mana Gharun<sup>1</sup>, Ankit Shekhar<sup>2</sup>, Lukas Hörtnagl<sup>2</sup>, Luana Krebs<sup>2</sup>, Nicola Arriga<sup>3</sup>, Mirco  
4 Migliavacca<sup>3</sup>, Marilyn Roland<sup>4</sup>, Bert Gielen<sup>4</sup>, Leonardo Montagnani<sup>5</sup>, Enrico Tomelleri<sup>5</sup>,  
5 Ladislav Šigut<sup>6</sup>, Matthias Pechl<sup>7</sup>, Peng Zhao<sup>7</sup>, Marius Schmidt<sup>8</sup>, Thomas Grünwald<sup>9</sup>, Mika  
6 Korkiakoski<sup>10</sup>, Annalea Lohila<sup>10</sup>, Nina Buchmann<sup>2</sup>

7

8 <sup>1</sup> Institute of Landscape Ecology, University of Münster, Germany

9 <sup>2</sup> Department of Environmental Systems Science, Institute of Agricultural Sciences, ETH  
10 Zurich, Switzerland

11 <sup>3</sup> European Commission, Joint Research Centre (JRC), Ispra, Italy

12 <sup>4</sup> Plants and Ecosystems (PLECO), Department of Biology, University of Antwerp, 2610  
13 Wilrijk, Belgium

14 <sup>5</sup> Free University of Bolzano, Faculty of Agricultural, Environmental and Food Sciences,  
15 39100 Bolzano, Italy

16 <sup>6</sup> Global Change Research Institute CAS, Bělidla 986/4a, CZ-60300 Brno, Czech Republic,  
17 ORCID: 0000-0003-1951-4100

18 <sup>7</sup> Department of Forest Ecology and Management, Swedish University of Agricultural  
19 Sciences (SLU), SE-901 83 Umeå, Sweden

20 <sup>8</sup> Agrosphere (IBG-3), Institute of Bio- and Geosciences, Jülich Research Centre, 52425  
21 Jülich, Germany

22 <sup>9</sup> Institute of Hydrology and Meteorology, Technical University of Dresden, Dresden,  
23 Germany

24 <sup>10</sup> Finnish Meteorological Institute, Climate System Research, Helsinki Finland

25

26 Corresponding author: Mana Gharun ([mana.gharun@uni-muenster.de](mailto:mana.gharun@uni-muenster.de))

27

28

29

**Abstract**

30 Relative to drought and heat waves, the effect of winter warming on forest CO<sub>2</sub> fluxes during  
31 the dormant season has less been investigated, despite its relevance for net CO<sub>2</sub> uptake in colder  
32 regions with higher carbon content in soils. Our objective was to test the effect of the  
33 exceptionally warm winter in 2020 on the winter CO<sub>2</sub> budget of cold-adapted evergreen needle-  
34 leaf forests across Europe, and identify the contribution of soil and air temperature to changes  
35 in winter CO<sub>2</sub> fluxes in response to warming. Our hypothesis was that warming in winter leads  
36 to higher emissions across colder sites due to increased ecosystem respiration. To test this  
37 hypothesis, we used 98 site-year eddy covariance measurements across 14 evergreen needle-  
38 leaf forests (ENFs) distributed from north to south of Europe (from Sweden to Italy). We used  
39 a data-driven approach to quantify the effect of air and soil temperature on changes in net  
40 ecosystem productivity (NEP) during the warm winter of 2020. Our results showed that the  
41 impact of warming was different across sites, as in the lower altitude and lower latitude sites  
42 positive soil temperature anomalies were larger, while positive air temperature anomalies were  
43 larger in the northern latitude and high-altitude sites. Warming in winter led to a divergent



44 response across the sites. Out of 14 sites only in 3 sites net ecosystem productivity declined in  
45 winter significantly in response to warming. In addition, we observed that in the colder sites  
46 daytime NEP (that is dominated by photosynthesis) declined with warming of the air in winter,  
47 whereas in the warmer sites daytime NEP increased with warming of the soil. While warming  
48 increases ecosystem respiration, it might not trigger productivity in winter if the soil within the  
49 rooting zone remains frozen. Forests within the same plant functional type category can exhibit  
50 differing reactions to winter warming and to predict their responses accurately it is crucial to  
51 account for variations in local climate, physiology, and structure simultaneously.

52

53 **Keywords:** eddy covariance, respiration, productivity, long-term, extremes, carbon flux

54

55

56

## 57 **Introduction**

58 One of the largest sources of uncertainties in understanding how forests can mitigate climate  
59 change is the variation of forest CO<sub>2</sub> fluxes in response to extreme climatic conditions. Forests  
60 absorb a large part of anthropogenic CO<sub>2</sub> emissions (Friedlingstein et al. 2023), but extreme  
61 climatic conditions compromise the capacity of forests for carbon sequestration (Shekhar et al.  
62 2023). While a large body of research focuses on extreme events during the growing season,  
63 effects of warming winters remain understudied (Kreyling et al. 2019). In northern latitudes  
64 and higher altitudes where evergreen conifers dominate, warming events are especially  
65 pronounced during the winter months (IPCC 2014). In 2020, Europe experienced its warmest  
66 winter on record since 1981 and the largest difference relative to the reference period (1981–  
67 2020) was observed in winter over northeastern Europe (Copernicus Climate Change Service  
68 2020). However, it is not clear yet how such winter warming affected winter CO<sub>2</sub> fluxes  
69 particularly where forests are covered by snow and with high soil C content. Understanding the  
70 impact of winter warming on forest net CO<sub>2</sub> uptake requires high temporal resolution  
71 observations (sub-seasonal, daily) across many regions, as mechanisms that control forest  
72 carbon fluxes are complex and show different responses to changes in climatic conditions,  
73 depending on the region and forest type.

74 At the tree level, winter warming could increase CO<sub>2</sub> uptake in temperature-limited forests.  
75 While little of this uptake is expected to be allocated to stem growth (Krejza et al. 2022), this  
76 increased activity can impact physiological development of plants that are adapted to long cold  
77 periods. Plant CO<sub>2</sub> uptake is controlled by a range of physiological responses to light,  
78 temperature and CO<sub>2</sub> concentrations. In addition to these external drivers, physiological factors  
79 (e.g., photosynthetic parameters such as light-use efficiency, maximum rate of electron



80 transport, maximum carboxylation rate, formation of carbohydrate reserves) and structural  
81 characteristics (e.g., leaf area index) which vary across different evergreen needle-leaf forests  
82 (ENF), directly affect how productivity and CO<sub>2</sub> uptake might be affected by warming in winter  
83 (Martinez Vilalta et al. 2016; Stocker et al. 2018).

#### 84 *Importance of winter period for evergreen needle-leaf forests (ENF)*

85 Forests adapted to cold environments require a persistent number of days with low temperatures  
86 for building hardiness. Sudden warming during winter months can promote vegetation activity  
87 in response to a condition similar to a “false spring” which can interrupt the cold hardiness  
88 process (Laube et al. 2014). Additionally, increased respiration due to warming can deplete  
89 stored non-structural carbohydrates (NSC) and tree hydraulic functioning (if combined with  
90 drought) and affect tree functioning in spring (Sperling et al. 2015). Winter warming also affects  
91 phenological development of trees and increases the chance of photo-oxidative frost damage  
92 during earlier stages of the growing season (Gu et al. 2008; Chamberlain et al. 2019). All of  
93 this would compromise the capacity of the forest for CO<sub>2</sub> uptake throughout the year (Desai et  
94 al. 2016).

95 Environmental cues such as temperature, photoperiod, and light quality control a network of  
96 signalling pathways that coordinate cold acclimation and cold hardiness in trees that ensure  
97 survival during long periods of low temperature and freezing (Öquist and Hünler 2003;  
98 Ensminger et al. 2006). These signalling pathways include the gating of cold responses by the  
99 circadian clock, the interaction of light quality and photoperiod, and the involvement of  
100 phytohormones in low temperature acclimation (Chang et al. 2021). Soluble carbohydrates,  
101 including sucrose (most abundant) accumulate in response to low temperatures, starting from  
102 late autumn throughout winter (Strimbeck & Schaberg 2009; Chang et al. 2015). Persistent  
103 uninterrupted cold periods thus play an important role in forming the photosynthetic capacity  
104 of the trees and their functioning under extreme climatic conditions. Experimental evidence  
105 from temperature-sensitive conifers shows that warm spells in winter can induce premature  
106 dehardening of buds, and result in stunted shoot development in the following spring (Nørgaard  
107 Nielsen & Rasmussen, 2008). In addition to damage from frost, earlier dehardening can  
108 potentially affect the capacity of trees to cope with a range of extreme climatic conditions such  
109 as cold spells, drought and heat waves.

#### 110 *Effect of warming on forest carbon fluxes*

111 Forest net ecosystem productivity (NEP) depends on the balance between gross ecosystem CO<sub>2</sub>  
112 uptake (gross primary productivity, GPP) and ecosystem respiration (Reco). Both these flux  
113 components are highly sensitive to climate drivers (e.g., air and soil temperature, solar



114 radiation), and thus when canopy structural changes from one year to another are negligible,  
115 the interannual variations can be predominantly explained by changes in the climatic conditions  
116 (Hui et al. 2003). Net ecosystem productivity can increase or decrease with changes in air  
117 temperature. In temperature-limited ecosystems for example, increase in air temperature  
118 increases photosynthesis which leads to a larger gross productivity and potentially increased  
119 net CO<sub>2</sub> uptake (if respiration does not increase more). However with warming and increased  
120 temperatures, respiration (autotrophic and heterotrophic) can also increase, and the balance of  
121 this with changes in gross productivity could lead to an increase, no change, or a reduction in  
122 net CO<sub>2</sub> uptake (Gharun et al. 2020). In the presence of winter warming, despite more  
123 favourable conditions for photosynthesis, factors such as water stress or photoinhibition caused  
124 by high photon flux densities in combination with low air temperatures could downregulate  
125 photochemical efficiency and negatively affect net photosynthesis which could decline gross  
126 primary productivity (Troeng and Linder 1982).

127 The temperature sensitivity of ecosystem respiration regulates how the terrestrial CO<sub>2</sub>  
128 emissions respond to a warming climate. Within naturally occurring temperature ranges,  
129 ecosystem respiration (sum of autotrophic and heterotrophic respirations) typically shows an  
130 exponential increase with temperature (Lloyd and Taylor 1994). While previous studies have  
131 shown an increase in Q<sub>10</sub> (times of increased soil respiration with a 10 °C increase of  
132 temperature) with decrease in site mean temperature (e.g., Chen et al. 2020), the temperature  
133 sensitivity of ecosystem respiration incorporates both the direct response of ecosystem  
134 respiration to temperature and indirect influences from other climatic and physiological  
135 variables such as moisture, leaf area index, photosynthate input, litter quality, microbial  
136 community (Reichstein et al. 2002; Fierer et al. 2005; Lindroth et al. 2008; Migliavacca et al.  
137 2011; Karhu et al. 2014; Collalti et al. 2020). These factors change across species composition  
138 and climatic regions and make predicting changes in forest carbon fluxes in response to  
139 warming challenging.

140 The winter of 2019-2020 was reported as the hottest on record (1981-2022) across Europe  
141 (Copernicus Climate Change Service/ECMWF). When compared to the average conditions, up  
142 to 45 less winter ice days were detected in eastern Europe Russe (C3S/KNMI). In Finland, for  
143 example, the average air temperature for January and February was over 6 degrees higher than  
144 the 1981-2010 mean (Copernicus Climate Change Service/ECMWF). In this study we  
145 investigated how the exceptionally warm winter of 2019-2020 affected ENFs in Europe. Our  
146 objectives were to:



147 1) evaluate the relative change in air and soil temperature during the winter 2019-2020,  
148 compared to a 6-year reference period of 2014-2019, 2) quantify the relative changes in the  
149 winter CO<sub>2</sub> fluxes across coniferous sites with available ecosystem-level CO<sub>2</sub> flux  
150 measurements, and 3) identify the contribution of climatic drivers (air temperature, soil  
151 temperature, solar radiation) to changes in CO<sub>2</sub> fluxes during the warm winter. Our hypothesis  
152 was that warming in winter leads to a larger negative effect on net CO<sub>2</sub> balance (i.e., higher  
153 emissions) across colder forests. We addressed these objectives and tested our hypothesis by  
154 exploring ecosystem-level CO<sub>2</sub> fluxes measured with eddy covariance over 98 site-years in 14  
155 evergreen needle-leaf forests distributed from the Boreal to the Mediterranean regions.

156

## 157 **Material and Methods**

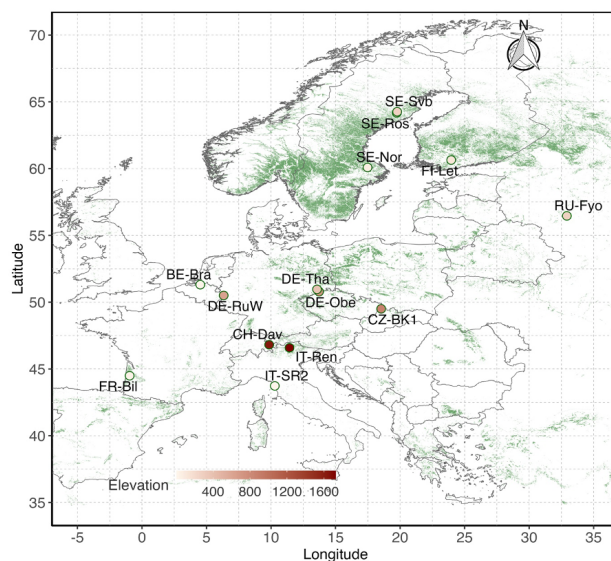
### 158 *Site description*

159 We selected 14 evergreen needle-leaf forests where continuous CO<sub>2</sub> fluxes and meteorological  
160 measurements were available for at least six years until the end of 2020. Selected sites were  
161 located from the northern to the southern edge of ENF forest distribution in Europe (Figure 1).

162

163 **Figure 1** Location of the 14 Evergreen Needleleaf Forest (ENF) sites included in this study.  
164 Base-map is the MODIS Land Cover Product (MOD12Q1, 500m spatial resolution) showing  
165 the distribution of ENFs in Europe in 2020. Elevation of the sites ranges from 4 m a.s.l. (IT-  
166 SR2) to 1735 m a.s.l. (IT-Ren).

167



168



169 The most northern site studied is located in Sweden at 64.2 °N (SE-Svb) and the most southern  
 170 site in Italy at 43.7 °N (IT-SR2). Mean annual air temperature varies between 1.8 °C (in SE-Ros  
 171 and SE-Svb) and 15.4 °C (in IT-SR2) across sites. Mean annual total precipitation varies from 527  
 172 mm (in SE-Nor) to 1316 mm (in CZ-BK1). Elevation ranges from 4 m a.s.l. (IT-SR2) to 1730 m  
 173 a.s.l. (IT-Ren). Table 1 summarizes the description of sites including their dominant canopy  
 174 species.

175

176 **Table 1** Description of the 14 ENF study sites. Mean annual temperature and total precipitation  
 177 refer to the 2014-2019 period. Mean number of days with snow cover for each site is based on  
 178 the MODIS satellite observations. Sites are listed in a decreasing order in the mean annual  
 179 temperature.

180

Site ID	Lat. (°)	Long. (°)	Altitude (m a.s.l.)	Canopy species (dominant first)	Mean annual temperature (°C)	Mean annual precipitation (mm)	Nr days with snow cover
IT-SR2	43.702	10.290	4	<i>Pinus pinea</i>	15.7	950	0
FR-Bil	44.493	-0.956	39	<i>Pinus pinaster</i>	14.1	930	11
BE-Bra	51.307	4.519	16	<i>Pinus sylvestris</i>	11.5	750	20
DE-Tha	50.962	13.565	385	<i>Picea abies</i>	10.2	843	41
DE-RuW	50.504	6.331	610	<i>Picea abies</i>	8.7	1250	50
DE-Obe	50.786	13.721	734	<i>Picea abies</i>	7.4	996	90
SE-Nor	60.086	17.479	45	Mixed ( <i>Pinus sylvestris</i> , <i>Picea abies</i> )	7.2	527	89
CZ-Bk1	49.502	18.536	875	<i>Picea abies</i>	7.1	1316	71
RU-Fyo	56.461	32.922	265	Mixed ( <i>Picea abies</i> , <i>Betula pubescens</i> )	6.1	711	58
FI-Let	60.641	23.959	111	Mixed ( <i>Pinus sylvestris</i> , <i>Picea abies</i> , <i>Betula pubescens</i> )	5.9	627	99
IT-Ren	46.586	11.433	1735	<i>Picea abies</i>	5.5	809	112
CH-Dav	46.815	9.855	1639	<i>Picea abies</i>	4.8	1062	139
SE-Ros	64.172	19.738	160	<i>Pinus sylvestris</i>	4.0	614	102
SE-Svb	64.256	19.774	267	Mixed ( <i>Pinus sylvestris</i> , <i>Picea abies</i> , <i>Betula pubescens</i> )	3.2	614	106

181

## 182 Dataset

183 We used the Warm Winter 2020 eddy covariance dataset processed with FLUXNET pipeline  
 184 (compatible with the FLUXNET2015 collection) in this study (Warm Winter 2020 Team, & ICOS  
 185 Ecosystem Thematic Centre, 2022); <https://www.icos-cp.eu/data-products/2G60-ZHAK>  
 186 (Pastorello et al. 2020). We included the analysis of the spring season at each site to account for



187 the responses immediately after the winter season. Winter months included December, January,  
188 and February and spring months included March, April, and May. The 6-year reference period was  
189 from 2014 to 2019. This period was selected to have sufficient temporal overlap between the sites.  
190 NEE quality-checked with a constant friction velocity ( $u^*$ ) threshold was used for all sites  
191 (NEE\_CUT\_REF)(Shekhar et al. 2023). For an easier interpretation, we present net ecosystem  
192 exchange as net ecosystem productivity (NEP = -NEE) where a negative NEP indicates that forest  
193 is a net source, and positive NEP indicates forest is a net sink of CO<sub>2</sub> (Chapin et al. 2006).  
194 In terms of climatic variables we selected those that overlapped across all sites during the study  
195 period. These included incoming shortwave radiation ( $R_g$ ), air temperature ( $T_{air}$ ), soil temperature  
196 at 5cm ( $T_{soil}$ ), precipitation and top soil water content. Given that continuous long-term snow depth  
197 measurements were not available at all sites, we used remotely sensed snow depth products to  
198 quantify mean snow depth and snow depth anomalies in winter 2020. The snow depth data were  
199 derived from the simulation of the Famine Early Warning Systems Network (FEWS NET) Land  
200 Data Assimilation System (FLDAS) (McNally et al., 2017). FLDAS data are produced from the  
201 Noah version 3.6.1 Land Surface Model (LSM) at a monthly resolution with a global coverage at  
202 a spatial resolution of  $0.1^\circ \times 0.1^\circ$  (approx.  $10 \text{ km} \times 10 \text{ km}$ ) (Kumar et al., 2013) and has been used  
203 in the past to study global spatiotemporal patterns of snow depth and cover (Notarnicola 2022).  
204 For snow cover we used MODIS/Terra (MOD10A2) and MODIS/AQUA (MYD10A2) (Hall and  
205 Riggs, 2021) Snow Cover 8-Day L3 Global 500m SIN Grid, Version 6 dataset, which provides  
206 maximum snow cover extent at 8-day temporal resolution and 500m spatial resolution. For each  
207 forest site, we derived average (2014-2019) leaf area index (LAI) from the LAI Collection 300 m  
208 Version 1.1 product (LAI300) provided by the Copernicus Global Land Service (Fuster et al.,  
209 2020). Average LAI was estimated for each site during the mean net CO<sub>2</sub> uptake period  
210 (Supplementary Figure 2). Start of the net carbon uptake period was defined as when daily NEP  
211 crosses from negative to positive, and end is the inverse.

### 212 *Statistical analysis*

213 We compared average daily and daytime (when  $R_g > 10 \text{ W/m}^2$  and local time 8-18h) means of  
214 each variable ( $v$ ; climate drivers, CO<sub>2</sub> fluxes) during the winter and spring of 2020 to the mean  
215 from a 6-year reference period (2014-2019) using a t-test ( $p < 0.05$ ). Daily means of each variable  
216 was calculated only using the measured and good quality gap-filled half-hourly data (variable  
217 quality control = 0 or 1). To understand the major drivers of winter and spring NEP for each forest  
218 site, we derived conditional variable importance (CVI <sub>$v$</sub> ) of each predictor variable ( $R_g$ ,  $T_{air}$ , and  
219  $T_{soil}$ ) based on a random forest regression model (Breiman, 2001). Soil water content was removed





220 from the drivers analysis because of its negligible effect on the overall model. We tuned the  
221 random forest model by iterating ‘ntree’ parameter (number of trees to grow) from 100 to 500 with  
222 steps of 50, and ‘mtry’ parameter (number of variables to try at each split) from 1 to 3 with steps  
223 of 1, and chose the parameter (ntree = 300 and mtry = 2) with the minimum mean square error.  
224  $CVI_v$  accounts for the correlation between the predictor variables, and was calculated using the  
225 *party* R-package (Hothorn et al., 2006). Based on a 7-day moving window (centered on the central  
226 value of the window) we calculated the mean daily (and daytime) NEP,  $T_{air}$ ,  $R_g$ , and  $T_{soil}$ . To  
227 compare the  $CVI_v$  across sites, for each site we calculated the relative CVI (RCVI) for each  
228 variable as per equation 2.

$$229 \quad RCVI_v (\%) = \frac{CVI_v}{\sum CVI_v} \times 100 \quad \text{Equation 2}$$

230 Where  $\sum CVI_v$  is the sum of  $CVI_v$  of all variables used in the model. We expressed changes in  
231 variable during 2020 ( $v_{2020}$ ) and the reference period ( $v_{reference}$ ) based on its relative anomaly  
232 ( $\Delta v_r$ ) and absolute anomaly ( $\Delta v_a$ ) as per equations 3 & 4.

$$233 \quad \Delta v_r (\%) = \frac{v_{2020} - v_{reference}}{|v_{reference}|} \times 100 \quad \text{Equation 3}$$

$$234 \quad \Delta v_a = v_{2020} - v_{reference} \quad \text{Equation 4}$$

235 To further understand the how (absolute) anomalies of different variables (daytime  $R_g$ ,  $T_{air}$ ,  $T_{soil}$ )  
236 explained the variation in daytime  $\Delta NEP$ , we used the RCVI (as per equation 2) derived from  
237 (also) a random forest regression model with hyperparameters  $ntree = 100$  and  $mtry = 3$  (tuned  
238 for lowest mean squared error), for each site (number of data points at least 80 days). The %  
239 variance explained of the model was based on the out-of-bag estimates.

240

## 241 **Results**

### 242 *Warm winter 2019-2020 conditions across different sites*

243 According to the *in-situ* data, compared to the reference period (2014-2019), winter 2020 was the  
244 warmest winter across 10 sites. In seven sites, the winter also had lower precipitation than normal  
245 (Figure 2, and Supplementary Figure 1). Positive air temperature anomalies in winter 2020 were  
246 larger in the high latitude or high-altitude sites compared to the mid-latitude and low-elevation  
247 sites (Figure 3) with largest anomaly of 4.79 °C in RU-Fyo and lowest positive anomaly of 0.87  
248 °C observed in IT-SR2 (Figure 3). The average number of snow cover days per year was highly





249 variable across the study sites. (Table 1). The southernmost site studied here (IT-SR2) typically  
250 has no snow cover in winter, while the subalpine forest in Switzerland (CH-Dav) has on average  
251 139 days with snow (Table 1). In those sites with consistent snow cover in winter (11 out of 14  
252 sites) snow depth declined at 9 out of 11 sites during the warm winter of 2020 and reduction was  
253 considerable in FI-Let, RU-Fyo, SE-Nor, DE-Obe, DE-Ruw, and DE-Tha (Figure 4). In SE-Svb,  
254 FI-Let and DE-Obe soil temperature at 5 cm was continuously above the freezing level in winter  
255 2020 (Figure 5), unlike the mean conditions at the sites where soil temperature fluctuates around  
256 zero in winter. Changes in winter temperature were more significant in winter than in spring  
257 (Figure 3), which is the reason why we focus on the effect of winter warming on CO<sub>2</sub> fluxes only.

#### 258 *Effect of climate drivers on winter CO<sub>2</sub> fluxes*

259 The annual net productivity of ENFs varied from being a maximum sink ( $\pm$ sd) of 797 ( $\pm$  320) g C  
260 m<sup>-2</sup> yr<sup>-1</sup> (CZ-BK1) to a maximum source of -311 ( $\pm$  93) g C m<sup>-2</sup> yr<sup>-1</sup> (SE-Nor) during the six-year  
261 reference period (2014-2019) (Table 2). Inter-annual variation in NEP was largest in CZ-BK1 (320  
262 gC m<sup>-2</sup> yr<sup>-1</sup>) and lowest in SE-Svb (35 gC m<sup>-2</sup> yr<sup>-1</sup>) (Table 2). The length of the net CO<sub>2</sub> uptake  
263 period was on average 178 days but varied between the sites from 105 days (in RU-Fyo) to 315  
264 days (in DE-Ruw) (Table 2, Suppl. Figure 2). Except FR-Bil and DE-RuW all sites were a CO<sub>2</sub>  
265 source in winter under reference conditions, however in IT-SR2, the forest shifted from a CO<sub>2</sub>  
266 source into a CO<sub>2</sub> sink in winter 2020 (Supplementary Table 1).

267 During the warm winter 2020, mean daily NEP (i.e., annual winter CO<sub>2</sub> sink or source strength)  
268 changed significantly ( $p < 0.05$ ) in 9 out of 14 sites (BE-Bra, CZ-BK1, DE-Obe, FI-Let, IT-Ren,  
269 IT-SR2, SE-Svb, SE-Nor, RU-Fyo, grouped as the “affected” sites) compared to the 2014-2019  
270 reference period, with changes in both positive and negative directions (Figure 6). For example,  
271 in BE-Bra, DE-Obe, IT-Ren, SE-Svb and FI-Let, the forest became a significantly larger source  
272 of CO<sub>2</sub> in winter 2020, while in IT-SR2, SE-Nor, CZ-BK1, and RU-Fyo forest shifted towards  
273 being a smaller source for CO<sub>2</sub> in winter 2020 (Figure 6, Supplementary Table 1). IT-SR2 showed  
274 the largest increased daily NEP in winter (346%) and BE-Bra showed the largest negative anomaly  
275 in daily NEP (-97%) (Figure 6). During the warm winter ecosystem respiration (approximated by  
276 nighttime NEP) increased significantly across 10 out of 14 sites (Figure 6). Daytime NEP however  
277 (dominated by productivity) increased significantly with warming in only 5 sites, and mainly in  
278 the warmer sites (Figure 6).

279 The relative importance results of the random forest regression analysis showed that across tested  
280 variables,  $R_g$  generally had the largest control on NEP. However, with decrease in site baseline  
281 (i.e., mean) temperature, the effect of  $R_g$  declined (Figure 7). For example, in the three coldest

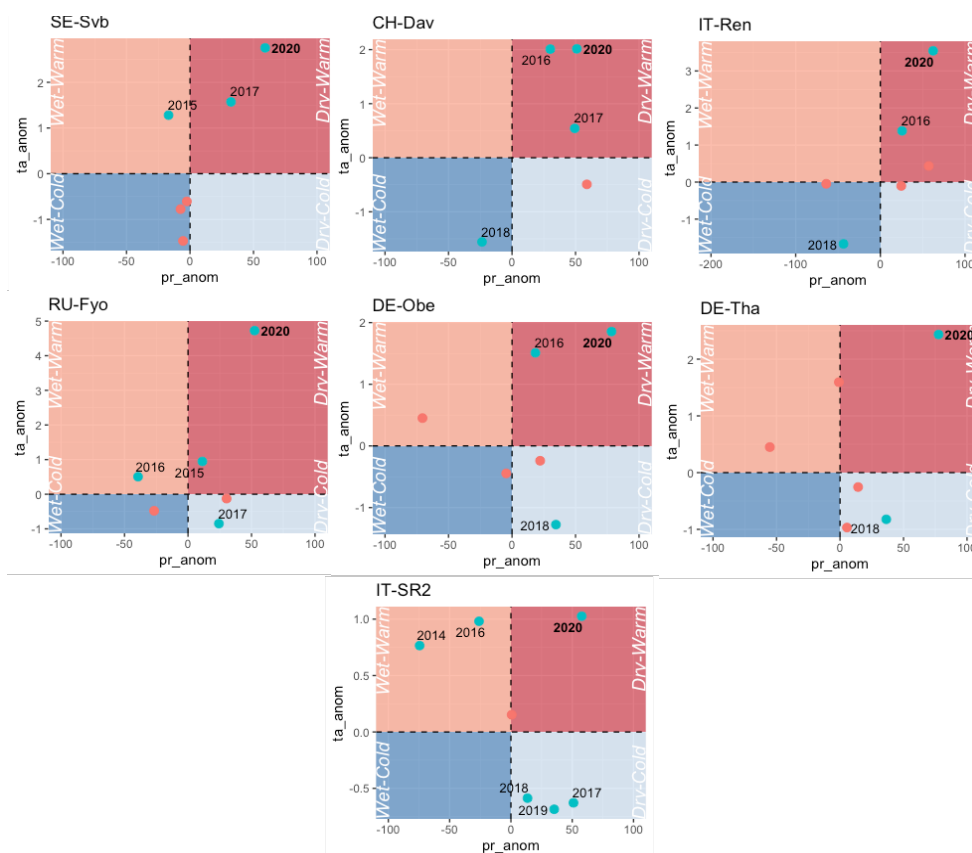


282 sites (SE-Svb, CH-Dav, IT-Ren)  $R_g$  had a relative importance of 52%, 23% and 41% for the  
283 variations in NEP respectively, while in the three warmest sites (IT-SR2, FR-Bil and BE-Bra)  $R_g$   
284 had a relative importance of 73%, 81% and 58% for NEP respectively (Figure 7). Radiation  
285 dominated the effect on winter GPP and temperature dominated the effect on winter respiration  
286 fluxes. Particularly in the colder sites the effect of radiation was the least (Figure 7).

287

288

289 **Figure 2** Winter temperature and precipitation anomalies ( $x\_anom = x - x\_mean$ ) in 2020 (between  
290 December 2019 and February 2020) at those sites where winter 2020 was the warmest and driest  
291 relative to winters during the reference period 2014-2019. Precipitation anomalies are converted  
292 to relative change (relative to mean) but temperature changes are in the original unit (°C).  
293 Anomalies are classified in four main classes of “wet-warm”, “dry-warm”, “wet-cold”, and “dry-  
294 cold”. Winter 2020 is marked in bold. Symbols are marked in blue and label (year) is displayed  
295 only if precipitation change was larger than 10% and at the same time temperature change more  
296 than 0.5 °C. Sites ordered by increasing mean temperature (SE-Svb coldest and IT-SR2 warmest).  
297  
298



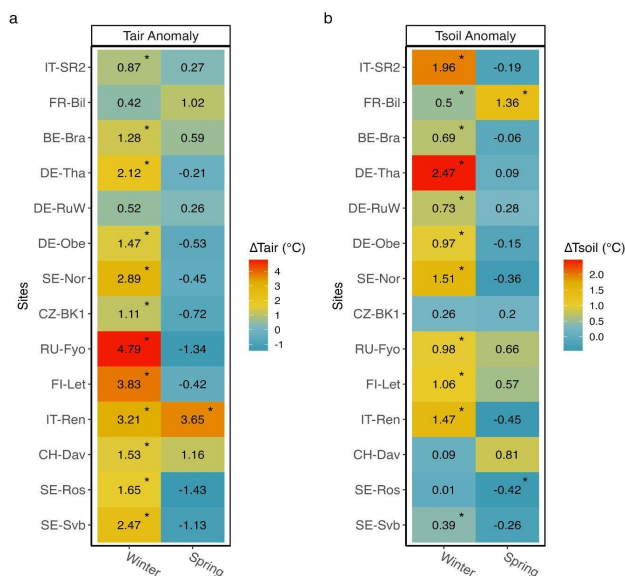
299

300

301



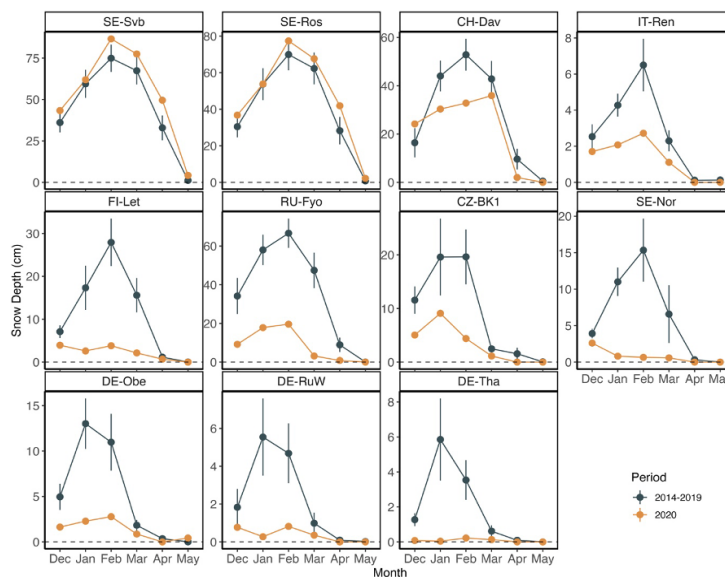
302 **Figure 3** Seasonal changes in air temperature ( $T_{air}$ ) and soil temperature ( $T_s$ ) in 2020 compared to  
 303 the 6-year reference period (2014-2019). Asterisk marks where means in 2020 were significantly  
 304 different from the reference period ( $p < 0.05$ ). Anomalies were calculated from daily values. Sites  
 305 are listed in a decreasing order of mean annual air temperature.



306

307

308 **Figure 4** December to May snow depth changes (cm) in winter 2020 compared to the average  
 309 winters during the reference period (2014-2019). Note that only 11 out of 14 sites have persistent  
 310 snow cover in winter. Sites ordered by increasing mean temperature (SE-Svb coldest and DE-  
 311 Tha warmest).  
 312



313



314 **Table 2** Mean total annual net ecosystem productivity (NEP) and the standard deviation (inter-  
 315 annual variation) during the reference period (2014 and 2019). Start of the net carbon uptake  
 316 period (SOS, day of year, DOY) is when daily NEP changes from negative to positive and end  
 317 (EOS) is the inverse (see Suppl. Figure 2). Sites are listed in a decreasing order in mean annual  
 318 air temperature.  
 319

Site ID	NEP ( $\pm$ sd) (g C m <sup>-2</sup> y <sup>-1</sup> )	SOS (DOY)	EOS (DOY)	Net carbon uptake period (days)
IT-SR2	197 ( $\pm$ 67)	35	200	165
FR-Bil	324 ( $\pm$ 103)	20	215	195
BE-Bra	279 ( $\pm$ 158)	95	270	175
DE-Tha	484 ( $\pm$ 88)	55	305	250
DE-Ruw	597 ( $\pm$ 155)	1	365	365
DE-Obe	251 ( $\pm$ 147)	75	265	190
SE-Nor	-311 ( $\pm$ 93)	90	200	110
CZ-Bk1	797 ( $\pm$ 320)	70	310	240
RU-Fyo	25 ( $\pm$ 50)	95	200	105
FI-Let	-113 ( $\pm$ 123)	100	230	130
IT-Ren	675 ( $\pm$ 70)	75	305	230
CH-Dav	231 ( $\pm$ 139)	80	280	200
SE-Ros	320 ( $\pm$ 136)	95	255	160
SE-Svb	163 ( $\pm$ 35)	95	240	145

320

321

322 *Effect of warming on NEP anomalies*

323 Across the low latitude or low altitude (< 1000 m a.s.l.) sites where NEP changed significantly  
 324 in winter 2020 (IT-SR2, BE-Bra, DE-Obe), average NEP anomaly was +75%. In the high-  
 325 latitude-high elevation sites where NEP was significantly different in winter 2020 (SE-Nor,  
 326 CZ-BK1, RU-Fyo, FI-Let, IT-Ren, SE-Svb) the average NEP anomaly was -8.8% (reduced net  
 327 uptake) (Figure 6, Supplementary Figure 5). Average variable explained by the random forest  
 328 regression for daytime  $\Delta$ NEP when abiotic drivers were included in winter was 72% in winter  
 329 (Figure 8). Across the affected sites, changes in the air temperature dominated the effect on  
 330 NEP anomalies (Figure 8). While FI-Let was affected by a partial cut in 2016 (Korkiakoski et  
 331 al. 2019; Korkiakoski et al. 2020), winter fluxes remained relatively stable in all pre- and post-  
 332 harvest years as the partial cut affected mostly the summer fluxes (data not shown here).  
 333 The relationship between air and soil temperature was stronger than radiation and air  
 334 temperature across sites and the relationship between air and soil temperature was stronger in  
 335 warmer sites (Table 3). In addition to snow cover, leaf area index and the degree of canopy  
 336 closure (directly related to LAI) affect the relationship between air and soil temperature through  
 337 a stronger shading of the soil in dense forests. CZ-BK1 had the largest LAI ( $4.52 \pm 0.09$  se)



338 and SE-Ros the smallest ( $2.59 \pm 0.09$ ). FI-Let had the largest inter-annual variation ( $\pm 0.27$ )  
 339 in LAI and IT-Ren and FR-Bil smallest inter-annual variation ( $\pm 0.08$ ) (Table 3).

340

341 **Table 3** Pearson correlation coefficient between mean daily incoming shortwave  
 342 radiation ( $R_g$ ), air temperature ( $T_{air}$ ) and soil temperature at 5m ( $T_{soil}$ ) at each site during  
 343 the reference period (2014-2019). Sites are ordered by a decreasing mean air  
 344 temperature. Leaf area index (LAI) values are shown as mean across the study period  $\pm$   
 345 standard error of the mean.

346

Site ID	$R_g$ - $T_{air}$	$T_{air}$ - $T_{soil}$	LAI $\pm$ se
IT-SR2	0.69	0.97	3.12 (0.11)
FR-Bil	0.65	0.76	3.50 (0.08)
BE-Bra	0.67	0.92	4.42 (0.13)
DE-Tha	0.73	0.96	4.04 (0.19)
DE-RuW	0.59	0.83	2.99 (0.22)
DE-Obe	0.72	0.94	3.69 (0.21)
SE-Nor	0.71	0.90	3.08 (0.09)
CZ-Bkl	0.72	0.92	4.52 (0.09)
RU-Fyo	0.74	0.78	4.06 (0.14)
FI-Let	0.66	0.88	3.29 (0.27)
IT-Ren	0.64	0.84	3.54 (0.08)
CH-Dav	0.63	0.87	3.25 (0.12)
SE-Ros	0.69	0.77	2.59 (0.09)
SE-Svb	0.71	0.84	2.79 (0.12)

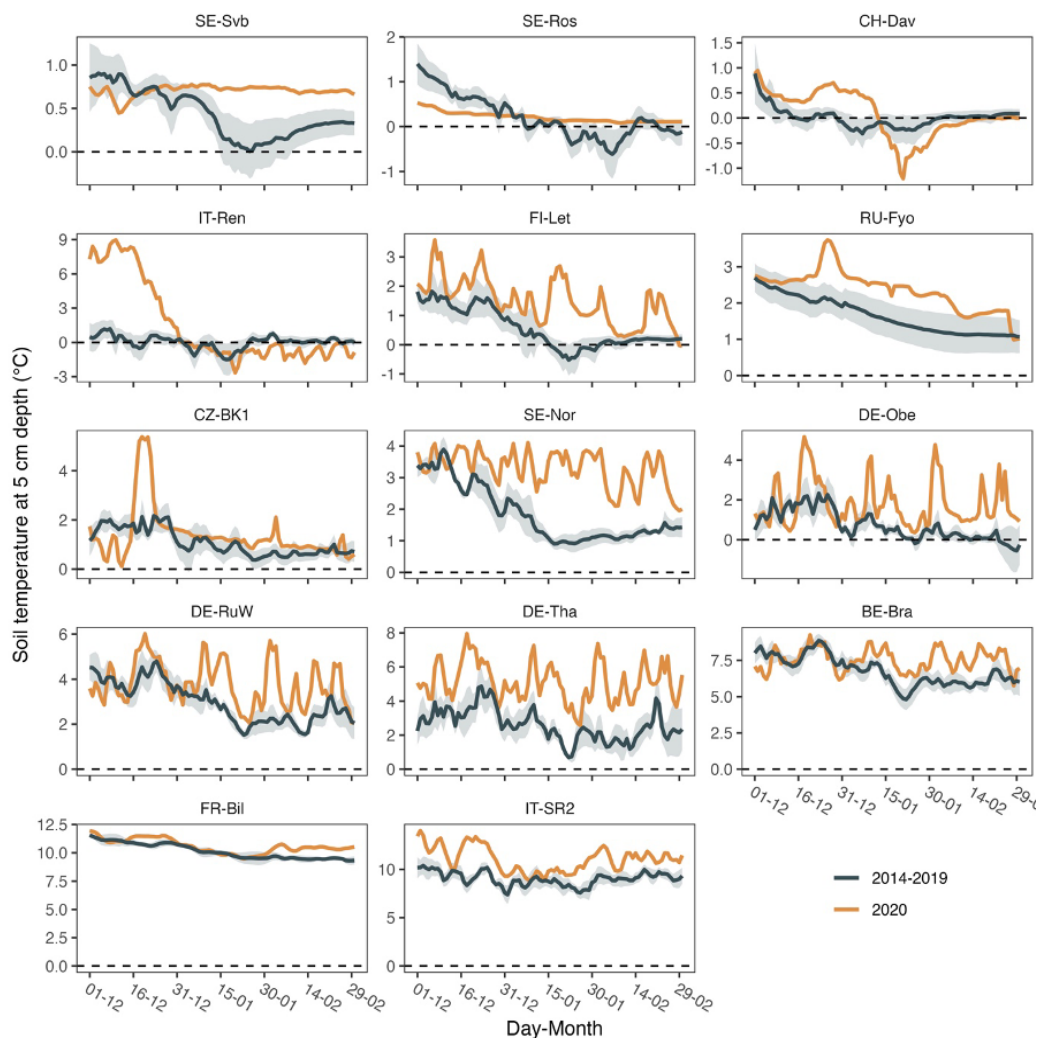
347

348

349

350 **Figure 5** Soil temperature (at 5cm) changes in winter 2020 compared to the reference period  
 351 (2014-2019). Shaded bands around the mean show the 95% confidence interval of mean soil  
 352 temperature. Sites are ordered (top and right to left) by increasing baseline temperature (SE-  
 353 Svb coldest and IT-SR2 warmest).

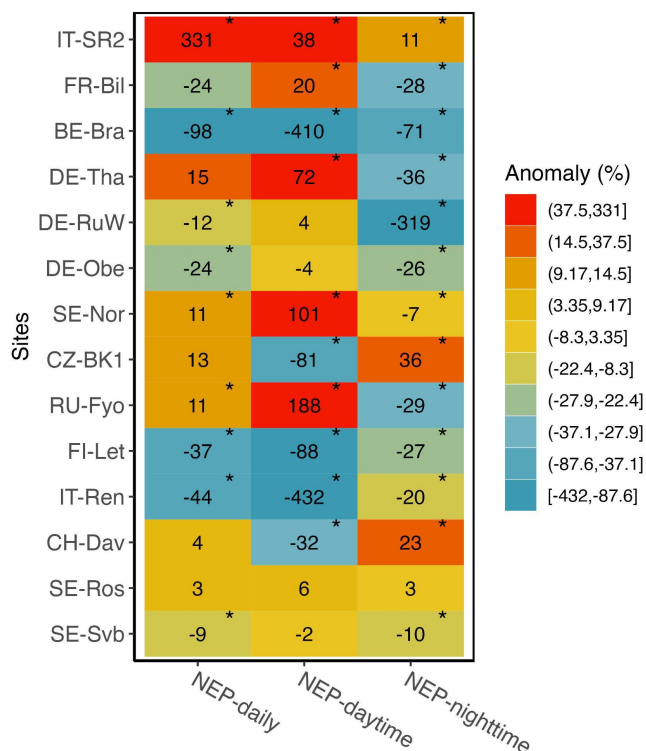
354



355  
356  
357  
358  
359  
360  
361  
362  
363  
364  
365  
366  
367  
368  
369



370 **Figure 6** Relative changes (%) in mean daily, nighttime, and daytime NEP in winter 2020  
 371 compared to the 6-year reference winters (2014-2019). Asterisks mark where means in 2020  
 372 were significantly different from the reference period ( $p < 0.05$ ). Positive NEP change indicates  
 373 increased net uptake (due to increased uptake or reduced emission) and negative change  
 374 indicates decreased net uptake (due to reduced uptake or increased emission). Sites are listed  
 375 in a decreasing mean annual air temperature order.  
 376

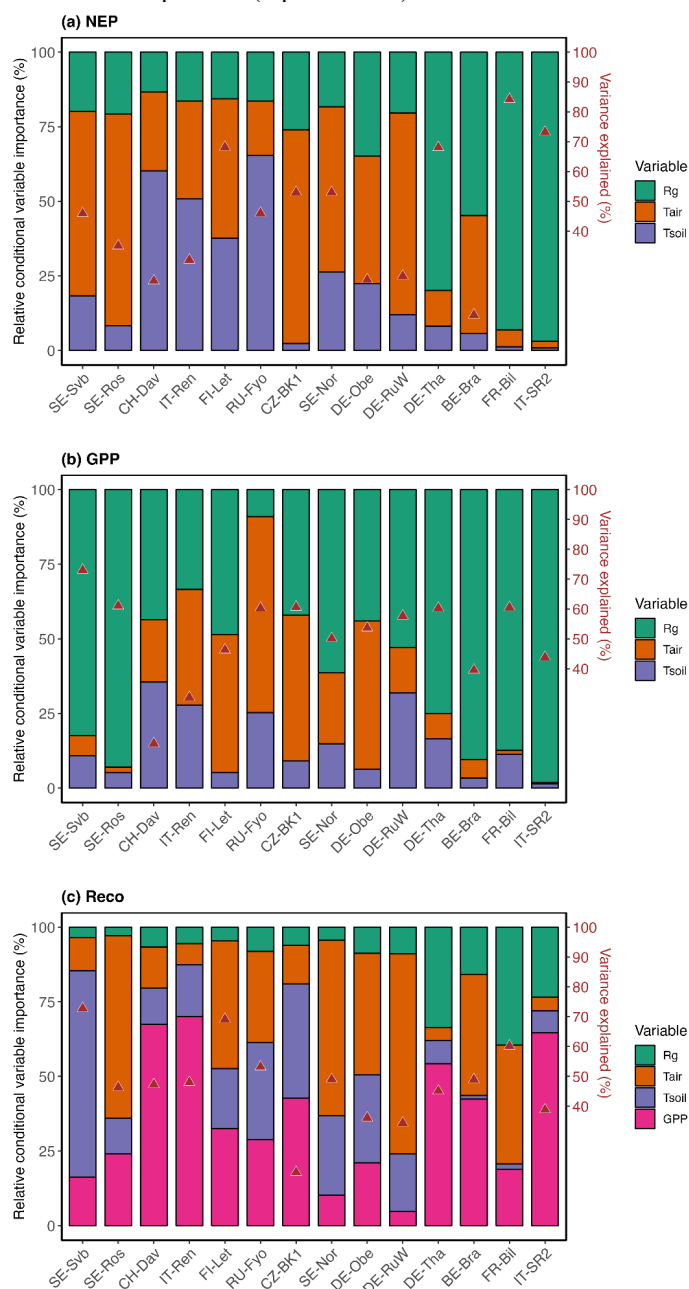


377  
 378  
 379  
 380  
 381  
 382  
 383  
 384  
 385  
 386  
 387  
 388  
 389  
 390  
 391  
 392  
 393





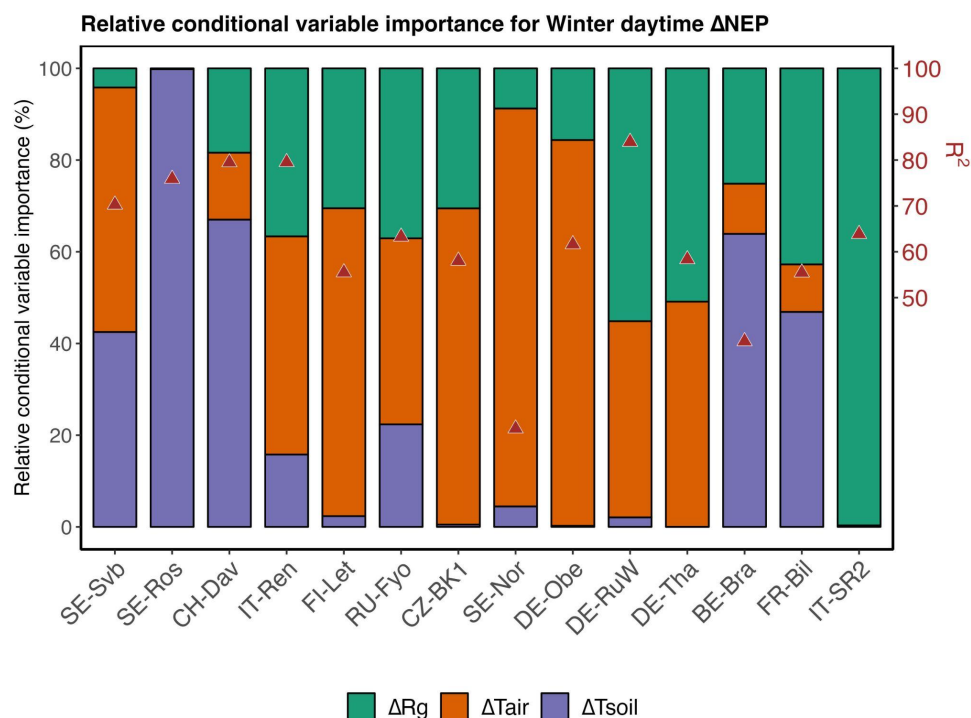
394 **Figure 7** Relative conditional variable importance (RCVI, %) of three climatic variables for  
 395 daily winter NEP, GPP and Reco, and the overall variable explained (marked with red  
 396 triangles) estimated from the random forest regression analysis. The RFR model was trained  
 397 on winter observations during the reference period (2014-2019). The sites are ordered by  
 398 decreasing mean annual temperature (top to bottom).



399  
400



401 **Figure 8** Comparison of the relative importance of abiotic ( $T_{air}$ ,  $R_g$ ,  $T_s$ ) variables, for NEP  
 402 changes ( $\Delta NEP$ ) in winter 2020.  $R^2$  of the RFR model that was used to explain the variation  
 403 in daytime  $\Delta NEP$  (i.e., when PPFD > 0) is shown on the secondary (right) y-axis and marked  
 404 with red triangles. Sites are ordered by increasing mean air temperature (from left to right).  
 405



406  
 407  
 408  
 409

## Discussion

### *Warming of the air and the soil in winter*

410 We tested how climate variables and  $CO_2$  fluxes deviated from a reference period (2014-2019)  
 411 during the warm winter of 2020, across 14 evergreen needle-leaf forest sites distributed from  
 412 north to south of Europe (from Sweden to Italy). The sites where winter 2020 was particularly  
 413 warm and dry were not clustered in a certain climatic region, however we observed a consistent  
 414 pattern that warming of the air was more pronounced in the northern latitude and on high  
 415 altitudes sites, while in lower latitudes and altitudes warming of the soil was more pronounced  
 416 (Figure 3). While in forests top soil temperature is directly affected by changes in the air  
 417 temperature, several underlying processes and properties modify the magnitude of decoupling  
 418 of air and soil temperature which could reach up to 10 degrees, depending on the season and  
 419 properties of the biome type (Lembrechts et al. 2022). These underlying factors and processes  
 420



421 include for example 1) a vertically complex and horizontally continuous forest structure that  
422 leads to higher decoupling of the soil temperature from air temperature, 2) soil moisture content  
423 as moisture increases the soil heat storage, 3) insulation by the litter or snow cover, 4) cloud  
424 cover, ground surface albedo, and rate of evapotranspiration which collectively affect the  
425 radiation balance and energy exchange between the soil and the air, and 5) microtopography  
426 that affects the drainage of air (e.g., cool air drains in low-lying areas) (Guan et al., 2009;  
427 Lozano-Parra et al., 2018; De Frenne et al., 2021; Gril et al., 2023). Given that in our study the  
428 type of forest was similar across sites (all sites were dominated by evergreen needle-leaf  
429 forests) and given that our focus was on the warming during the winter season, we attribute the  
430 main source of difference in the soil and air temperature to two main factors. First the snow  
431 depth that ranged from no snow to over 100 cm across sites (Table 1, Figure 4), and second,  
432 differences in forest structure (e.g. LAI) which varied between 2.59 to 4.52 across the sites  
433 (Table 3). We observed that the sites with the smaller snow depth showed a larger warming of  
434 the soil during the warm winter of 2020 perhaps because the insulating effect of snow cover  
435 was weaker here (Friesen et al. 2021) (Figure 2, Figure 4). At the sites where snow depth  
436 declined significantly in winter 2020, soil temperatures increased substantially with large  
437 fluctuations over the season, whereas in other sites with greater snow depth such soil  
438 temperature fluctuations were absent (Figure 5). The link between warming of the air and  
439 warming of the soil was also controlled by the canopy structure as we found a significant  
440 positive relationship between the two ( $p < 0.05$ ,  $r = 0.69$ ). Although the direct effect of canopy  
441 closure on snow distribution, accumulation and melting at different periods was not tested here,  
442 it was evident that sites that had a larger LAI also showed a tighter coupling between air  
443 temperature and soil temperature as forest canopy closure reduces snow depth (Table 3)(Woods  
444 et al. 2006; Gao et al. 2022).

#### 445 *Winter warming effect on forest CO<sub>2</sub> fluxes*

446 Our general observation was that across sites with a lower mean average temperature (i.e., high  
447 altitude or high latitude sites) winter warming was concurrent with increased net CO<sub>2</sub>  
448 emissions. In the warmer sites however (low altitude or low latitude sites) winter warming also  
449 increased the productivity and CO<sub>2</sub> uptake (Supplementary Figure 5). This difference can  
450 generally be explained by the balance of changes in the warming of the soil versus warming of  
451 the air (Bond-Lamberty and Thomson 2010) which affects both soil respiration and tree CO<sub>2</sub>  
452 uptake. Where soil becomes proportionally warmer and soil temperature reaches above  
453 freezing levels, root activity is enhanced and tree productivity responds directly to the increased



454 air temperatures, and CO<sub>2</sub> uptake increases. Warming of the air - if not translated into a direct  
455 warming of the soil- might not enhance productivity if the soil within the rooting zone remains  
456 frozen. In IT-Ren for example where daytime NEP declined significantly in the warm winter,  
457 air temperature increased to over 3.5 degrees more than normal, however soil temperature  
458 remained at freezing levels (Figure 5).

459 CO<sub>2</sub> fluxes are sensitive to changes in both temperature and light (e.g., incoming radiation) and  
460 site baseline climate conditions showed to be a good proxy of how changes in light and air  
461 temperature lead to changes in NEP (Figure 7). There is however evidence that temperature  
462 responses of biochemical processes are a function of plant growth temperature, and not just  
463 instantaneous temperature (Fürstenau Togashi et al. 2018). In addition, response of NEP to  
464 similar temperature can be different across seasons (i.e., an evident hysteresis), depending on  
465 other environmental factors such as solar radiation and soil water content (Niu et al. 2011).  
466 While across different sites sensitivity of NEP to temperature increases with a decrease in site  
467 mean temperature, as site mean temperature increases (temperature is no longer limiting)  
468 radiation becomes a larger constraint on NEP (Running et al. 2004).

469 Chamber-based observations from boreal forests show that snow-depth and soil moisture affect  
470 temperature sensitivity of soil CO<sub>2</sub> fluxes as the freeze-thaw cycles abruptly change the  
471 moisture content of the soil (Du et al., 2013). In that sense, warmer winters can trigger larger  
472 respiration (and availability of nutrients to trees) because of higher Q<sub>10</sub> of thawed than frozen  
473 soils (Wang et al., 2014), however microbial C limitation can reduce expected increase in  
474 respired CO<sub>2</sub>, if not countered by greater labile C inputs (Sullivan et al., 2020). In addition,  
475 aboveground productivity increases with increase in temperature (Supplementary Figure 3) and  
476 enhances the autotrophic respiration. Warming in winter also affects the microbial community  
477 that control labile and stable organic carbon decomposition in the soil that would offset  
478 respiration response to temperature and lead to a reduction of soil respiration under warming  
479 (Tian et al., 2021). The magnitude of increase in belowground autotrophic respiration in  
480 response to warming and the supply of labile substrate through rhizodeposition and root  
481 exudate also affects net CO<sub>2</sub> fluxes under warming (Nyberg et al., 2020). Decrease in the snow  
482 pack and increased soil freezing has short-term immediate impacts on plant CO<sub>2</sub> uptake, but  
483 can also leave a long-lasting negative impact on functioning of trees (Repo et al. 2021).  
484 Particularly sites with prolonged cold winter seasons could be rather negatively affected by the  
485 warming in winter, as we observed through reduced daytime NEP which is an indication of  
486 stress from warming during winter. Trees growing in northern latitudes and higher altitudes  
487 could be more negatively affected by warming in winter as optimal temperatures in trees are



488 regulated by the short-term changes in temperature, whereas in ecosystems where temperature  
489 fluctuations are seasonally larger, optimal temperature for growth has a broader range (Weng  
490 et al. 2010; Liu 2020).

491

#### 492 *Winter tree physiology effect on CO<sub>2</sub> fluxes*

493 Responses of coniferous species to soil warming can vary largely depending on the species'  
494 adaptive traits, the overall ecosystem context, and interactions with other environmental factors  
495 such as precipitation, temperature, and nutrient availability (Dawes et al. 2017; Oddi et al.  
496 2022). The sites we studied here, although all were dominated by evergreen needle-leaf species,  
497 consisted of different canopy species and some sites were dominated by a mixture of species  
498 (Table 1). There can be significant differences in photosynthetic parameters across different  
499 species of evergreen conifers that would affect tree and ecosystem response to warming  
500 (Fürstenau Togashi et al. 2018). The different responses of productivity to increased warming  
501 in ENFs can stem from differences in the quantity (and quality) of stored NSC in the roots, and  
502 the rate at which this C storage is mobilized within the tree during the warm winter (Bansal  
503 and Germino 2009). Warmer temperatures and dry conditions in winter lead to stomatal closure  
504 and depletion of carbohydrate reserves for trees that are adapted to ample precipitation and low  
505 VPD conditions in winter, and this effect leads to reduced CO<sub>2</sub> uptake of trees during warmer  
506 winters (Earles et al. 2018).

507 Low temperature is essential for signals that trigger the synthesis of soluble carbohydrates  
508 involved in osmotic and freezing protection against cold extremes (Chang et al. 2021) that  
509 otherwise impair the Calvin cycle by inhibiting the regeneration of ribulose biphosphate  
510 (RuBP) and decrease the efficiency of Rubisco carboxylation (Ensminger et al. 2012; Crosatti  
511 et al. 2013). Non-structural carbohydrates (sugar and starch) that are accumulated during the  
512 growing season are utilized in winter to ensure survival of trees (Zhu et al. 2012; Tixier et al.  
513 2020) and failure to develop overwintering defences can cause evergreen conifer needles to  
514 remain susceptible for example to photo-oxidative damage during frost events (Chang et al.  
515 2016).

516 Our results provide the first analysis of the effect of winter warming on CO<sub>2</sub> fluxes of evergreen  
517 needle-leaf forests in Europe and point to the importance of understanding multiple underlying  
518 mechanisms that govern CO<sub>2</sub> fluxes. Data on the responses of photosynthetic traits on a  
519 timescale that is ecologically relevant (days to years) are scarce, but eddy covariance  
520 observations provide an opportunity for constructing long-term time series of canopy level



521 processes to investigate the effect of extreme climatic conditions across all seasons. We  
522 encourage studies that combine long-term observations and plant-level experiments to  
523 investigate how changes in the functioning in winter might affect trees' response to extremes  
524 that occur earlier in the growing season (e.g., spring frost, spring drought) and to understand  
525 the consequences of such extremes for ecosystem carbon uptake.

526

### 527 **Conclusion**

528 Our study investigated the effect of winter warming on CO<sub>2</sub> fluxes of evergreen needle-leaf  
529 forests across Europe during the warm 2019-2020 winter. We found significant differences in  
530 the impact of warming across sites, with northern and higher-altitude locations experiencing  
531 more significant warming of the air, while southern and lower-altitude sites saw greater soil  
532 warming. Winter warming influenced forest CO<sub>2</sub> fluxes, with daytime Net Ecosystem  
533 Productivity (NEP) decreasing in colder sites due to lower soil temperature, while warmer sites  
534 experienced increased CO<sub>2</sub> uptake. However, responses were not similar across all sites, and  
535 factors such as forest structure, and local mean climatic conditions played a role in creating  
536 microclimates that buffer or enhance the impact of warming on CO<sub>2</sub> fluxes. Understanding  
537 these variations combined with tree ecophysiological functioning of cold-adapte ecosystems is  
538 crucial for predicting how forests will respond to future winter warming.

539

### 540 **Acknowledgements**

541 MG acknowledges funding from the Swiss National Science Foundation project ICOS-CH  
542 Phase 3 (20FI20\_198227). TG acknowledges funding from Free State of Saxony (project  
543 'Sicherstellung des Treibhausgasmonitorings an sächsischen ICOS-Standorten') and BMBF  
544 (project ICOS-D building phase). BG and RM acknowledge the Research Foundation Flanders  
545 (FWO) for the support of ICOS research infrastructure. NB acknowledges funding from the  
546 SNF for ICOS-CH Phase 2 (20FI20\_173691), and EcoDrive (IZCOŽ0\_198094). LŠ was  
547 supported by the Ministry of Education, Youth and Sports of CR within the CzeCOS program,  
548 grant number LM2023048. We acknowledge the ICOS research infrastructure for data  
549 provision.

550

551 *Data availability:* The dataset used in this study is openly available from the ICOS  
552 Carbon Portal. <https://doi.org/10.18160/2G60-ZHAK>

553

554 *Author contributions:* MG designed the study; MG and AS performed the data analysis;  
555 MG wrote the manuscript, and all authors commented on the analysis and contributed  
556 substantially to the writing of the manuscript.

557

558 *Competing interests:* The authors declare that they have no conflict of interests.



559 **References**

- 560 Bansal S, Germino MJ (2009) Temporal variation of nonstructural carbohydrates in montane  
561 conifers: similarities and differences among developmental stages, species and  
562 environmental conditions. *Tree Physiology* 9(4), 559-568, DOI:  
563 10.1093/treephys/tpn045
- 564 Bond-Lamberty, B., Thomson, A. Temperature-associated increases in the global soil  
565 respiration record. *Nature* 464, 579–582 (2010). <https://doi.org/10.1038/nature08930>
- 566 Breiman, L. (2001). Random forests. *Machine Learning*, 45(1), 5–32.  
567 <https://doi.org/10.1023/A:1010933404324>
- 568 Chamberlain, C. J., Cook, B. I., García de Cortázar-Atauri, I., & Wolkovich, E. M. (2019).  
569 Rethinking false spring risk. *Global Change Biology*, 25(7), 2209-2220.  
570 doi:<https://doi.org/10.1111/gcb.14642>
- 571 Chang, C. Y., Unda, F., Zubilewich, A., Mansfield, S. D., & Ensminger, I. (2015). Sensitivity  
572 of cold acclimation to elevated autumn temperature in field-grown *Pinus strobus*  
573 seedlings. *Frontiers in Plant Science*, 6.
- 574 Chang, C. Y., Fréchette, E., Unda, F., Mansfield, S. D., & Ensminger, I. (2016). Elevated  
575 temperature and CO<sub>2</sub> stimulate late-season photosynthesis but impair cold hardening in  
576 pine. *plant physiology*, 172(2), 802-818.  
577 doi:10.1104/pp.16.00753doi:10.3389/fpls.2015.00165
- 578 Chang, C. Y.-Y., Bräutigam, K., Hüner, N. P. A., & Ensminger, I. (2021). Champions of  
579 winter survival: cold acclimation and molecular regulation of cold hardiness in  
580 evergreen conifers. *New Phytologist*, 229(2), 675-691.  
581 doi:<https://doi.org/10.1111/nph.16904>
- 582 Chapin, F.S., Woodwell, G.M., Randerson, J.T. et al. Reconciling Carbon-cycle Concepts,  
583 Terminology, and Methods. *Ecosystems* 9, 1041–1050 (2006).  
584 <https://doi.org/10.1007/s10021-005-0105-7>
- 585 Chen, J.L., Reynolds, J.F., Harley, P.C. et al. (1993) Coordination theory of leaf nitrogen  
586 distribution in a canopy. *Oecologia* 93, 63–69. <https://doi.org/10.1007/BF00321192>
- 587 Chen S, Wang J, Zhang T, Hu Z (2020) Climatic, soil, and vegetation controls of the  
588 temperature sensitivity (Q<sub>10</sub>) of soil respiration across terrestrial biomes. *Global*  
589 *Ecology and Conservation* 22, e00955
- 590 Collalti, A. et al. Plant respiration: controlled by photosynthesis or biomass? *Glob. Change*  
591 *Biol.* 26, 1739–1753 (2020).
- 592 Crosatti, C., Rizza, F., Badeck, F.-W., Mazzucotelli, E., & Cattivelli, L. (2013). Harden the  
593 chloroplast to protect the plant. *Physiologia Plantarum*, 147 1, 55-63.
- 594 Dawes, M.A., Schleppei, P., Hättenschwiler, S., Rixen, C. and Hagedorn, F. (2017), Soil  
595 warming opens the nitrogen cycle at the alpine treeline. *Glob Change Biol*, 23: 421-434.  
596 <https://doi.org/10.1111/gcb.13365>
- 597 De Frenne, P., Lenoir, J., Luoto, M., Scheffers, B.R., Zellweger, F., Aalto, J., Ashcroft, M.B.,  
598 Christiansen, D.M., Decocq, G., De Pauw, K., Govaert, S., Greiser, C., Gril, E., Hampe,  
599 A., Jucker, T., Klinges, D.H., Koelemeijer, I.A., Lembrechts, J.J., Marrec, R., Meeussen,  
600 C., Ogée, J., Tyystjärvi, V., Vangansbeke, P. and Hylander, K. (2021), Forest  
601 microclimates and climate change: Importance, drivers and future research agenda. *Glob*





- 602 Change Biol, 27: 2279-2297. <https://doi.org/10.1111/gcb.15569>
- 603 Desai A., G. Wohlfahrt, M.J. Zeeman, G. Katata, W. Eugster, L. Montagnani, D. Gianelle, M.  
604 Mauder and H-P Schmid (2016) Montane ecosystem productivity responds more to  
605 global circulation patterns than climatic trends. Environmental Research Letters, 11,  
606 024013.
- 607 Du E. et al., (2013) Winter soil respiration during soil-freezing process in a boreal forest in  
608 Northeast China, Journal of Plant Ecology, Volume 6, Issue 5, Pages 349–357,  
609 <https://doi.org/10.1093/jpe/rtt012>
- 610 Earles, J.M., Stevens, J.T., Sperling, O., Orozco, J., North, M.P. and Zwieniecki, M.A.  
611 (2018), Extreme mid-winter drought weakens tree hydraulic–carbohydrate systems and  
612 slows growth. New Phytol, 219: 89-97. <https://doi.org/10.1111/nph.15136>
- 613 Ensminger, I., Busch, F., & Huner, N. P. A. (2006). Photostasis and cold acclimation: sensing  
614 low temperature through photosynthesis. Physiologia Plantarum, 126(1), 28-44.  
615 doi:<https://doi.org/10.1111/j.1399-3054.2006.00627.x>
- 616 Ensminger, I., Berninger, F., & Streb, P. (2012). Response of photosynthesis to low  
617 temperature. In J. Flexas, F. Loreto, & H. Medrano (Eds.), Terrestrial photosynthesis in  
618 a changing environment: a molecular, physiological, and ecological approach (pp. 276–  
619 293): UK: Cambridge University Press.
- 620 Fierer, N., Craine, J. M., McLauchlan, K. & Schimel, J. P. Litter quality and the temperature  
621 sensitivity of decomposition. Ecology 86, 320–326 (2005).
- 622 Friedlingstein, P., O'Sullivan, M., Jones, M. W., Andrew, R. M., Bakker, D. C. E., Hauck, J.,  
623 Landschützer, P., Le Quéré, C., Luijckx, I. T., Peters, G. P., Peters, W., Pongratz, J.,  
624 Schwingshackl, C., Sitch, S., Canadell, J. G., Ciais, P., Jackson, R. B., Alin, S. R.,  
625 Anthoni, P., Barbero, L., Bates, N. R., Becker, M., Bellouin, N., Decharme, B., Bopp,  
626 L., Brasika, I. B. M., Cadule, P., Chamberlain, M. A., Chandra, N., Chau, T.-T.-T.,  
627 Chevallier, F., Chini, L. P., Cronin, M., Dou, X., Enyo, K., Evans, W., Falk, S., Feely,  
628 R. A., Feng, L., Ford, D. J., Gasser, T., Ghattas, J., Gkritzalis, T., Grassi, G., Gregor, L.,  
629 Gruber, N., Gürses, Ö., Harris, I., Hefner, M., Heinke, J., Houghton, R. A., Hurtt, G. C.,  
630 Iida, Y., Ilyina, T., Jacobson, A. R., Jain, A., Jarníková, T., Jersild, A., Jiang, F., Jin, Z.,  
631 Joos, F., Kato, E., Keeling, R. F., Kennedy, D., Klein Goldewijk, K., Knauer, J.,  
632 Korsbakken, J. I., Körtzinger, A., Lan, X., Lefèvre, N., Li, H., Liu, J., Liu, Z., Ma, L.,  
633 Marland, G., Mayot, N., McGuire, P. C., McKinley, G. A., Meyer, G., Morgan, E. J.,  
634 Munro, D. R., Nakaoka, S.-I., Niwa, Y., O'Brien, K. M., Olsen, A., Omar, A. M., Ono,  
635 T., Paulsen, M., Pierrot, D., Pockock, K., Poulter, B., Powis, C. M., Rehder, G.,  
636 Resplandy, L., Robertson, E., Rödenbeck, C., Rosan, T. M., Schwinger, J., Séférian, R.,  
637 Smallman, T. L., Smith, S. M., Sospedra-Alfonso, R., Sun, Q., Sutton, A. J., Sweeney,  
638 C., Takao, S., Tans, P. P., Tian, H., Tilbrook, B., Tsujino, H., Tubiello, F., van der Werf,  
639 G. R., van Ooijen, E., Wanninkhof, R., Watanabe, M., Wimart-Rousseau, C., Yang, D.,  
640 Yang, X., Yuan, W., Yue, X., Zaehle, S., Zeng, J., and Zheng, B.: Global Carbon Budget  
641 2023, Earth Syst. Sci. Data, 15, 5301–5369, <https://doi.org/10.5194/essd-15-5301-2023>,  
642 2023.
- 643 Friesen, H.C., Slesak, R.A., Karwan, D.L., Kolka, R.K., (2021) Effects of snow and climate  
644 on soil temperature and frost development in forested peatlands in Minnesota, USA.  
645 Geoderma 394, 115015.
- 646 Foyer, C.H., Neukermans, J., Queval, G., Noctor, G., Harbinson, J. (2012) Photosynthetic



- 647 control of electron transport and the regulation of gene expression. *J. Exp. Bot.*, 63, pp.  
648 1637-1661
- 649 Fürstenau Togashi, H., Prentice, I. C., Atkin, O. K., Macfarlane, C., Prober, S. M.,  
650 Bloomfield, K. J., and Evans, B. J. (2018) Thermal acclimation of leaf photosynthetic  
651 traits in an evergreen woodland, consistent with the coordination hypothesis,  
652 *Biogeosciences*, 15, 3461–3474, <https://doi.org/10.5194/bg-15-3461-2018>.
- 653 Fuster, B., Sánchez-Zapero, J., Camacho, F., García-Santos, V., Verger, A., Lacaze, R.,  
654 Weiss, M., Baret, F., & Smets, B. (2020). Quality assessment of PROBA-V LAI,  
655 fAPAR and fCOVER collection 300 m products of Copernicus global land service.  
656 *Remote Sensing*, 12(6), 1017. <https://doi.org/10.3390/rs1206101>
- 657 Gao, Y., Shen, L., Cai, R., Wang, A., Yuan, F., Wu, J., Guan, D., & Yao, H. (2022). Impact  
658 of Forest Canopy Closure on Snow Processes in the Changbai Mountains, Northeast  
659 China. *Frontiers in Environmental Science*, 10, Article 929309.  
660 <https://doi.org/10.3389/fenvs.2022.929309>
- 661 Gharun, M., Hörtnagl, L., Paul-Limoges, E., Ghiasi, S., Feigenwinter, I., Burri, S.,  
662 Marquardt, K., Etzold, S., Zweifel, R., Eugster, W., & Buchmann, N. (2020).  
663 Physiological response of Swiss ecosystems to 2018 drought across plant types and  
664 elevation. *Philosophical Transactions of the Royal Society B: Biological Sciences*,  
665 375(1810), 20190521. <https://doi.org/10.1098/rstb.2019.0521>
- 666 Gril, E., Spicher, F., Greiser, C., Ashcroft, M. B., Pincebourde, S., Durrieu, S., Nicolas, M.,  
667 Richard, B., Decocq, G., Marrec, R., & Lenoir, J. (2023). Slope and equilibrium: A  
668 parsimonious and flexible approach to model microclimate. *Methods in Ecology and*  
669 *Evolution*, 14, 885– 897. <https://doi.org/10.1111/2041-210X.14048>
- 670 Gu L, et al. (2008) The 2007 Eastern US Spring Freeze: Increased Cold Damage in a  
671 Warming World?, *BioScience*, Volume 58, Issue 3, March 2008, Pages 253–  
672 262, <https://doi.org/10.1641/B580311>
- 673 Guan, X., Huang, J., Guo, N. et al. (2009) Variability of soil moisture and its relationship  
674 with surface albedo and soil thermal parameters over the Loess Plateau. *Adv. Atmos.*  
675 *Sci.* 26, 692–700. <https://doi.org/10.1007/s00376-009-8198-0>
- 676 Hall, D. K. and G. A. Riggs. MODIS/Terra Snow Cover 8-Day L3 Global 500m SIN Grid,  
677 Version 6. 2021, Distributed by NASA National Snow and Ice Data Center Distributed  
678 Active Archive Center.
- 679 Hothorn, T., Hornik, K., and Zeileis, A.: Unbiased Recursive Partitioning: A Conditional  
680 Inference Framework, *J. Comput. Graph. Stat.*, 15, 651–674,  
681 <https://doi.org/10.1198/106186006X133933>, 2006.
- 682 Hui, D., Luo, Y., & Katul, G. (2003). Partitioning interannual variability in net ecosystem  
683 exchange between climatic variability and functional change. *Tree Physiology*, 23(7),  
684 433-442. doi:10.1093/treephys/23.7.433
- 685 IPCC, 2014: Climate Change 2014: Synthesis Report. Contribution of Working Groups I, II  
686 and III to the Fifth Assessment Report of the Intergovernmental Panel on Climate  
687 Change [Core Writing Team, R.K. Pachauri and L.A. Meyer (eds.)]. IPCC, Geneva,  
688 Switzerland, 151 pp.



- 689 Karhu, K., Auffret, M., Dungait, J. et al. Temperature sensitivity of soil respiration rates  
690 enhanced by microbial community response. *Nature* 513, 81–84 (2014).  
691 <https://doi.org/10.1038/nature13604>
- 692 Knauer, J., El-Madany, T. S., Zaehle, S., & Migliavacca, M. (2018). Bigleaf-An R package  
693 for the calculation of physical and physiological ecosystem properties from eddy  
694 covariance data. *PLoS ONE*, 13(8), e0201114. doi:10.1371/journal.pone.0201114
- 695 Korkiakoski M, Tuovinen JP, Penttilä T, Sarkkola S, Ojanen P, Minkkinen K, Rainne J,  
696 Laurila T, Lohila A (2019) Greenhouse gas and energy fluxes in a boreal peatland forest  
697 after clear-cutting, *Biogeosciences* 16, pp. 3703-3723, 10.5194/bg-16-3703-2019
- 698 Korkiakoski M, Ojanen P, Penttilä I, Minkkinen K, Sarkkola S, Rainne J, Laurila T, Lohila A  
699 (2020) Impact of partial harvest on CH<sub>4</sub> and N<sub>2</sub>O balances of a drained boreal peatland  
700 forest, *Agricultural and Forest Meteorology* 295, 108168,  
701 <https://doi.org/10.1016/j.agrformet.2020.108168>
- 702 Krejza, J., Haeni, M., Darenova, E., Foltýnová, L., Fajstavr, M., Světlík, J., ... Zweifel, R.  
703 (2022). Disentangling carbon uptake and allocation in the stems of a spruce forest.  
704 *Environmental and Experimental Botany*, 196, 104787,  
705 <https://doi.org/10.1016/j.envexpbot.2022.104787>
- 706 Kreyling, J., Grant, K., Hammerl, V. et al. (2019) Winter warming is ecologically more  
707 relevant than summer warming in a cool-temperate grassland. *Sci Rep* 9, 14632.  
708 <https://doi.org/10.1038/s41598-019-51221-w>
- 709 Kumar, S. V. et al. (2013) Multiscale evaluation of the improvements in surface snow  
710 simulation through terrain adjustments to radiation. *J. Hydrometeorol.* 14, 220–232.
- 711 Lasslop, G., Reichstein, M., Papale, D., Richardson, A., Arneeth, A., Barr, A., Stoy, P., and  
712 Wohlfahrt, G. (2010) Separation of net ecosystem exchange into assimilation and  
713 respiration using a light response curve approach: critical issues and global evaluation,  
714 *Glob. Change Biol.*, 16, 187–208, <https://doi.org/10.1111/j.13652486.2009.02041.x>
- 715 Laube, J. et al., Chilling outweighs photoperiod in preventing precocious spring development.  
716 *Glob. Change Biol.* 20, 170–182 (2014).
- 717 Lembrechts, J. J., van den Hoogen, J., Aalto, J., Ashcroft, M. B., De Frenne, P., Kemppinen,  
718 J., Kopecký, M., Luoto, M., Maclean, I. M. D., Crowther, T. W., Bailey, J. J., Haesen, S.,  
719 Klings, D. H., Niittynen, P., Scheffers, B. R., Van Meerbeek, K., Aartsma, P.,  
720 Abdalaze, O., Abedi, M., ... Lenoir, J. (2022). Global maps of soil temperature. *Global  
721 Change Biology*, 28, 3110– 3144. <https://doi.org/10.1111/gcb.16060>
- 722 Lindroth, A. et al. Leaf area index is the principal scaling parameter for both gross  
723 photosynthesis and ecosystem respiration of Northern deciduous and coniferous forests.  
724 *Tellus B* 60, 129–142 (2008).
- 725 Liu Y. (2020) Optimum temperature for photosynthesis: from leaf- to ecosystem-scale. *Sci  
726 Bull* 65(8):601-604. doi: 10.1016/j.scib.2020.01.006.
- 727 Lloyd J, Taylor JA (1994) On the temperature dependence of soil respiration. *Funct. Ecol.*, 8  
728 (1994), pp. 315-323



- 729 Lozano-Parra J, Pulido M, Lozano-Fondón C, Schnabel S. (2018) How do Soil Moisture and  
730 Vegetation Covers Influence Soil Temperature in Drylands of Mediterranean Regions?  
731 Water 10(12):1747. <https://doi.org/10.3390/w10121747>
- 732 Maire V, Martre P, Kattge J, Gastal F, Esser G, Fontaine S, et al. (2012) The Coordination of  
733 Leaf Photosynthesis Links C and N Fluxes in C3 Plant Species. PLoS ONE 7(6): e38345.  
734 <https://doi.org/10.1371/journal.pone.0038345>
- 735 Martinez Vilalta, J., Sala, A., Asensio, D., Galiano, L., Hoch, Gü., Palacio, S., Piper, F.,  
736 Lloret, F.. (2016). Dynamics of non-structural carbohydrates in terrestrial plants: A  
737 global synthesis. Ecological Monographs. 86. 10.1002/ecm.1231.
- 738 McNally, A. et al. (2017) A land data assimilation system for sub-Saharan Africa food and  
739 water security applications. Sci. Data 4, 170012. <https://doi.org/10.1038/sdata.2017.12>
- 740 Migliavacca, M. et al. Semiempirical modeling of abiotic and biotic factors controlling  
741 ecosystem respiration across eddy covariance sites. Glob. Change Biol. 17, 390–409  
742 (2011).
- 743 Niu S., Luo Y., Fei S., Montagnani L., Bohrer G., Janssens I.A., Gielen B., Rambal S.,  
744 Moors E., Matteucci G., (2011). Seasonal hysteresis of net ecosystem exchange in  
745 response to temperature change: patterns and causes. Global Change Biology, 17, 3102-  
746 3114, DOI: 10.1111/j.1365-2486.2011.02459.x.
- 747 Nørgaard Nielsen, C. C., & Rasmussen, H. N. (2008). Frost hardening and dehardening in  
748 *Abies procera* and other conifers under differing temperature regimes and warm-spell  
749 treatments. Forestry: An International Journal of Forest Research, 82(1), 43-59.  
750 doi:10.1093/forestry/cpn048
- 751 Notarnicola, C. Overall negative trends for snow cover extent and duration in global  
752 mountain regions over 1982–2020. Sci Rep 12, 13731 (2022).  
753 <https://doi.org/10.1038/s41598-022-16743-w>.
- 754 Nyberg, M. and Hovenden, M. J. (2020) Warming increases soil respiration in a carbon-rich  
755 soil without changing microbial respiratory potential, Biogeosciences, 17, 4405–4420,  
756 <https://doi.org/10.5194/bg-17-4405-2020>.
- 757 Öquist, G., & Huner, N. P. A. (2003). Photosynthesis of Overwintering Evergreen Plants.  
758 Annual Review of Plant Biology, 54(1), 329-355.  
759 doi:10.1146/annurev.arplant.54.072402.115741
- 760 Oddi et al (2022) Contrasting responses of forest growth and carbon sequestration to heat and  
761 drought in the Alps, Environ. Res. Lett. 17, 045015, doi:10.1088/1748-9326/ac5b3a
- 762 Pastorello, G., Trotta, C., Canfora, E. et al. The FLUXNET2015 dataset and the ONEFlux  
763 processing pipeline for eddy covariance data. Sci Data 7, 225 (2020).  
764 <https://doi.org/10.1038/s41597-020-0534-3>
- 765 Reichstein, M. et al. Ecosystem respiration in two Mediterranean evergreen holm oak forests:  
766 drought effects and decomposition dynamics. Funct. Ecol. 16, 27–39 (2002).
- 767 Repo, T., Domisch, T., Kilpeläinen, J. et al. Soil frost affects stem diameter growth of  
768 Norway spruce with delay. Trees 35, 761–767 (2021). <https://doi.org/10.1007/s00468-020-02074-8>
- 769



- 770 Running SW, Nemani RR, Heinsch FA, Zhao M, Reeves M, Hashimoto H (2004). A  
771 Continuous Satellite-Derived Measure of Global Terrestrial Primary Production,  
772 BioScience, Volume 54, Issue 6, Pages 547–560, [https://doi.org/10.1641/0006-3568\(2004\)054\[0547:ACSMOG\]2.0.CO;2](https://doi.org/10.1641/0006-3568(2004)054[0547:ACSMOG]2.0.CO;2)  
773
- 774 Shekhar, A., Hörtnagl, L., Buchmann, N., & Gharun, M. (2023). Long-term changes in forest  
775 response to extreme atmospheric dryness. *Global Change Biology*, 00, 1– 18.  
776 <https://doi.org/10.1111/gcb.16846>
- 777 Sperling, O., Earles, J.M., Secchi, F., Godfrey, J., Zwieniecki, M.A. (2015) Frost induces  
778 respiration and accelerates carbon depletion in trees. *PLoS ONE* 10(2): e0144124. doi:  
779 10.1371/journal.pone.0144124
- 780 Stocker, B.D., Zscheischler, J., Keenan, T.F., Prentice, I.C., Peñuelas, J. and Seneviratne, S.I.  
781 (2018), Quantifying soil moisture impacts on light use efficiency across biomes. *New*  
782 *Phytol*, 218: 1430-1449. <https://doi.org/10.1111/nph.15123>
- 783 Strimbeck, G. R., & Schaberg, P. G. (2009). Going to extremes: low temperature tolerance  
784 and acclimation in temperate and boreal conifers. In M. T. Gusta L.; Wisniewski, K.,  
785 (Ed.), *Plant cold hardiness: from the laboratory to the field* (pp. 226-239): Wallingford,  
786 Oxfordshire, UK: CABI Publishing.
- 787 Sullivan, P.F., Stokes, M.C., McMillan, C.K. et al. (2020) Labile carbon limits late winter  
788 microbial activity near Arctic treeline. *Nat Commun* 11, 4024.  
789 <https://doi.org/10.1038/s41467-020-17790-5>
- 790 Tian, J., Zong, N., Hartley, I.P., He, N., Zhang, J., Powlson, D., Zhou, J., Kuzyakov, Y.,  
791 Zhang, F., Yu, G. and Dungait, J.A.J. (2021), Microbial metabolic response to winter  
792 warming stabilizes soil carbon. *Glob Change Biol*, 27: 2011-2028.  
793 <https://doi.org/10.1111/gcb.15538>
- 794 Tixier, A., Guzmán-Delgado, P., Sperling, O. et al. Comparison of phenological traits, growth  
795 patterns, and seasonal dynamics of non-structural carbohydrate in Mediterranean tree  
796 crop species. *Sci Rep* 10, 347 (2020). <https://doi.org/10.1038/s41598-019-57016-3>
- 797 Troeng E, Linder S (1982) Gas exchange in a 20-year-old stand of Scots pine .1. Net  
798 photosynthesis of current and one-year-old shoots within and between seasons, *Physiol.*  
799 *Plant*. 54: 15-23.
- 800 Walker et al. (2014) The relationship of leaf photosynthetic traits –  $V_{max}$  and  $J_{max}$  – to leaf  
801 nitrogen, leaf phosphorus, and specific leaf area: a meta-analysis and modeling study.  
802 *Ecology and Evolution* 2014 4( 16): 3218– 3235
- 803 Warm Winter 2020 Team, & ICOS Ecosystem Thematic Centre. (2022). Warm Winter 2020  
804 ecosystem eddy covariance flux product for 73 stations in FLUXNET-Archive format—  
805 release 2022-1 (Version 1.0). ICOS Carbon Portal. <https://doi.org/10.18160/2G60-ZHAK>  
806
- 807 Wang, Y., et al. (2014), Non-growing-season soil respiration is controlled by freezing and  
808 thawing processes in the summer monsoon-dominated Tibetan alpine grassland, *Global*  
809 *Biogeochem. Cycles*, 28, 1081– 1095, doi:10.1002/2013GB004760.
- 810 Weng, Jen-Hsien & Liao, T.-S. (2010). Photosynthetic responses and acclimation to  
811 temperature in seven conifers grown from low to high elevations in subtropical Taiwan.  
812 *Taiwan Journal of Forest Science*. 25. 117-127.



- 813 Woods, S. W., Ahl, R., Sappington, J., and McCaughey, W. (2006). Snow Accumulation in  
814 Thinned Lodgepole Pine Stands, Montana, USA. *For. Ecol. Manag.* 235 (1-3), 202–211.  
815 doi:10.1016/j.foreco.2006.08.013
- 816 Wullschleger, S.D. (1993) Biochemical limitations to carbon assimilation in C3 plants - a  
817 retrospective analysis of the A/Ci curves from 109 species. *J. Exp. Bot.*, 44, pp. 907-920
- 818 Zhu WZ, Xiang JS, Wang SG, Li MH (2012) Resprouting ability and mobile carbohydrate  
819 reserves in an oak shrubland decline with increasing elevation on the eastern edge of the  
820 Qinghai-Tibet Plateau. *For Ecol Manage* 278:118–1